Homoclinic bifurcation properties near eight-figure homoclinic orbit

Yong-Kui Zou*

Department of Mathematics, Jilin University,

Changchun 130012, P. R. China. yzou@mail.jl.cn.

Abstract

In this paper we investigate the homoclinic bifurcation properties near a co-dimension two eight-figure homoclinic orbit of a planar dynamical system. The corresponding local bifurcation diagram is also illustrated by numerical computation.

Keywords: Eight figure homoclinic orbit, bifurcation diagram.
AMS Classification: Primary 65L10. Secondary 58F14, 34C37.

1 Introduction

In this paper we study the homoclinic bifurcation properties near an eight-figure homoclinic orbit of a planar dynamical system. If at a saddle equilibrium the four branches of the stable and unstable manifolds perform two single homoclinic orbits simultaneously, it is called an eight-figure homoclinic orbit. An example of such orbit is shown in Figure 1.1.

*This work was started while the author visited University of Cologne and Bielefeld during 1998-2001. He thanks Prof. Dr. T. Küpper and Prof. Dr. W.-J. Beyn for their stimulating discussion and kind entertainment. He also thanks Dr. F. Giannakopoulos for his helpful discussion.

Submitted to the Chinese Journal of Northeast Mathematics, November, 2000.

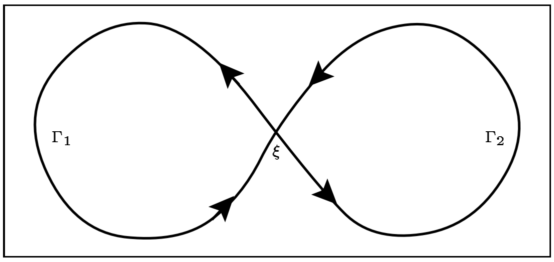

Figure 1.1 *An illustration of eight-figure homoclinic orbit.*

The eight-figure homoclinic orbit is a co-dimension 2 bifurcation phenomenon . Such orbit can lead to rich dynamics and appears in many literature, see [3, 5, 10, 9, 12, 13, 14, 8, 6, 7] and the references therein. The eight-figure homoclinic orbit also occurs in many applications.

In the paper [8], Guckenheimer studied a mathematical model for stirred tank reactor. This model consists of two ordinary differential equations with a polynomial nonlinearity. With the aid of numerical simulation and heuristic arguments, besides the global bifurcation properties he proved the existence of an eight-figure homoclinic orbit and he also provided a corresponding local bifurcation diagram.

In a small neural network consisting of two neurons (cf. [6]), Giannakopoulos and Oster also found an eight-figure homoclinic orbit. The bifurcation properties of periodic orbits nearby were well studied by numerical computation in this paper.

In the paper [7], Giannakopoulos, Küpper and Zou studied the global bifurcation properties of a planar system of a valve generator, which consists of an electronic valve and an oscillatory circuit. An eight-figure homoclinic orbit was found and its local bifurcation properties were studied by numerical experiments.

While studying the homoclinic bifurcation properties near an eight-figure homoclinic orbit, two different types of single homoclinic orbits are often involved. Usually there are four branches of the stable and unstable manifolds at a saddle equilibrium and one branch of stable manifolds and one branch of unstable manifolds coincide with each other to perform a single homoclinic orbit. If the other two branches of invariant manifolds lie outside of the region created by the homoclinic orbit we call it a small homoclinic orbit, see the left picture of Figure 1.2. Otherwise, if the other two branches are included in the interior of the homoclinic orbit we call it a big one, see the right picture in Figure 1.2.

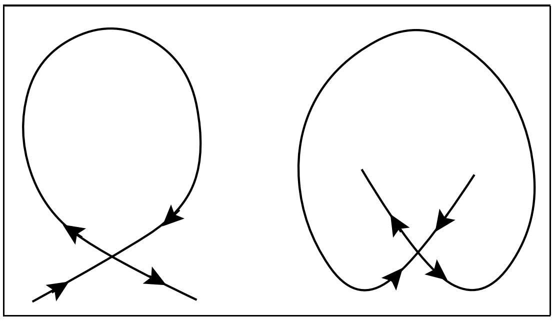

Figure 1.2 *Examples of a small and a big homoclinic orbits.*

It is easy to verify that there will bifurcate two families of small homoclinic orbits from the eight-figure homoclinic orbit under small perturbation. It has been observed from numerical experiments (cf. [8, 3, 5, 6, 7]) that the big homoclinic orbits also emanate from the eight-figure homoclinic orbit. But, to the author's knowledge there is no proof on the existence of the big homoclinic orbit near an eight-figure homoclinic orbit in the literature.

In this work, we will give a complete proof on the existence of small and big homoclinic orbits emanated from the eight-figure homoclinic orbit under small perturbation. To illustrate our results, we numerically investigate the local homoclinic bifurcation diagram near the eight-figure homoclinic of a chemical model studied by Guckenheimer in [8]. Then we compare our numerical bifurcation diagram with that in [8].

The organization of this paper follows. In section 2 we introduce and prove our main results on the existence of small and big homoclinic orbits near an eight-figure homoclinic orbit. Then in section 3 we introduce the numerical method for the computation and continuation of homoclinic orbits. At last, in section 4 we study the homoclinic bifurcation diagram near the eight-figure homoclinic orbit of a planar system studied in [8] with the aid of numerical computations.

2 Main results and proof

Consider a parameterized planar dynamical system

$$\dot{x} = f(x, \kappa, \eta), \quad x \in \mathbb{R}^2, \quad \kappa, \eta \in \mathbb{R}. \tag{2.1}$$

We assume

(H1) The function f is smooth enough.

(H2) ξ is a saddle equilibrium of equation (2.1) for all κ and η, i.e. $f(\xi, \kappa, \eta) = 0$ and $\det f_x(\xi, \kappa, \eta) < 0$.

(H3) At the parameter value $(\bar{\kappa}, \bar{\eta})$ equation (2.1) has two single small homoclinic orbits $\Gamma_1 = \{\bar{x}_1(t); t \in \mathbb{R}\}$ and $\Gamma_2 = \{\bar{x}_2(t); t \in \mathbb{R}\}$ which perform an eight-figure homoclinic orbit, see Figure 1.1.

(H4) The homoclinic orbits Γ_1 and Γ_2 are nondegenerate with respect to the parameters κ and η, respectively.

The nondegenerate property means that the Melnikov integral is nonzero, i.e.

$$\int_{-\infty}^{+\infty} y_i^T(t) f_\alpha(\bar{x}_i(t), \bar{\kappa}, \bar{\eta}) dt \neq 0 \tag{2.2}$$

where $\alpha = \kappa$ if $i = 1$, $\alpha = \eta$ if $i = 2$ and $y_i(t)$ is the unique bounded solution of the adjoint variational equation along the homoclinic orbit Γ_i

$$\dot{y}(t) + f_x(\bar{x}_i(t), \bar{\kappa}, \bar{\eta})^T y(t) = 0. \tag{2.3}$$

According to [4] and [15, Corollary 2.1], the nondegenerate homoclinic orbits can be continued by extra parameters.

Lemma 2.1 *Assume* (H1)–(H4). *Then there exist a constant $\delta > 0$ and functions $\kappa = \kappa_1(\eta)$ with $\bar{\kappa} = \kappa_1(\bar{\eta})$ and $\eta = \eta_2(\kappa)$ with $\bar{\eta} = \eta_2(\bar{\kappa})$, such that for $|\eta - \bar{\eta}| < \delta$ (resp. $|\kappa - \bar{\kappa}| < \delta$) and $\kappa = \kappa_1(\eta)$ (resp. $\eta = \eta_2(\kappa)$), equation* (2.1) *has a family of nondegenerate small homoclinic orbits $\Gamma_1(\eta) = \{\bar{x}_1^\eta(t), t \in \mathbb{R}\}$ (resp. $\Gamma_2(\kappa) = \{\bar{x}_2^\kappa(t), t \in \mathbb{R}\}$).*

By rotating the (κ, η)-axis in the parameter plane, we can have $\kappa_1'(\bar{\eta}) \neq 0$ and $\eta_2'(\bar{\kappa}) \neq 0$. Without loss of generality, we assume

(H5) $\kappa_1'(\bar{\eta}) > 0$ and $\eta_2'(\bar{\kappa}) < 0$.

From this assumption we know that the inverse function of $\kappa = \kappa_1(\eta)$ exists and we assume it is $\eta = \eta_1(\kappa)$ with $\bar{\eta} = \eta_1(\bar{\kappa})$. Then we denote the family of homoclinic orbits $\Gamma_1(\eta) = \{\bar{x}_1^{\eta}(t), t \in \mathbb{R}\}$ by $\Gamma_1(\kappa) = \{\bar{x}_1^{\kappa}(t), t \in \mathbb{R}\}$.

It has already been proved in [11] that the nondegenerate property implies transversal property for a planar homoclinic orbit. We assume that the transversal property of the homoclinic orbit Γ_1 and Γ_2 appears in the way shown in Figure 2.1 and Figure 2.2, respectively.

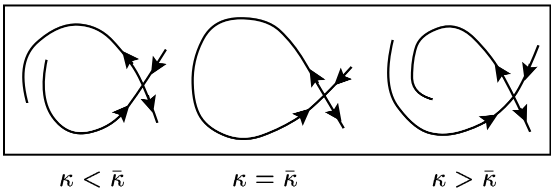

Figure 2.1 *The transversal property of homoclinic* Γ_1.

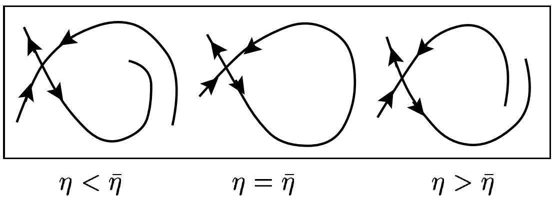

Figure 2.2 *The transversal property of homoclinic* Γ_2.

Throughout this paper, in all the bifurcation diagrams we always use κ as the horizontal axis and η as the vertical axis in the parameter plane.

Obviously, the families of homoclinic orbits $\Gamma_i(\kappa)$ $(i = 1, 2)$ preserve the same transversal structure while κ varies near $\bar{\kappa}$, which is shown in Figure 2.3.

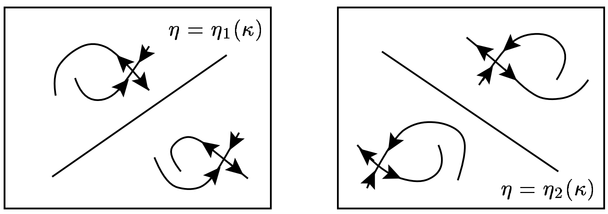

Figure 2.3 *The transversal properties of the families of homoclinic orbits* $\Gamma_1(\kappa)$ *and* $\Gamma_2(\kappa)$.

Now, we are ready to prove the existence of big homoclinic orbit near an eight-figure homoclinic orbit.

Choosing a crossing section to the homoclinic orbit Γ_2, see Figure 2.4. For any given $\kappa < \bar{\kappa}$, take $\eta = \eta_1(\kappa)$. Then the eight-figure homoclinic breaks in such a way that the single homoclinic orbit $\Gamma_1(\kappa)$ is preserved and the other single homoclinic orbit Γ_2 disappears in the way shown in the left picture of Figure 2.4. Assume the stable and unstable branches derived by the homoclinic Γ_2 intersect the crossing section at points a and c, respectively. If we choose $\tilde{\eta} > \eta_1(\kappa)$, the homoclinic orbit $\Gamma_1(\kappa)$ also breaks in the way shown in the right picture of Figure 2.4 and its unstable branch intersects the crossing section at a point b. If $\tilde{\eta} - \eta_1(\kappa)$ is small enough, the point b is very close to the point c (cf. [2]), hence the point b is at the left side of the point a, see the right picture in Figure 2.4.

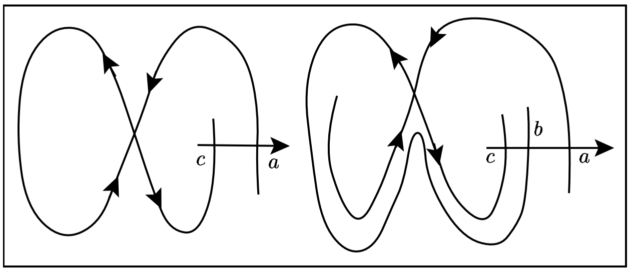

Figure 2.4 *One broken structure of the eight-figure homoclinic orbit.*

Similarly, we consider the broken manner of the eight-figure homoclinic orbit when $\eta = \eta_2(\kappa)$ and choosing $\tilde{\tilde{\eta}} < \eta_2(\kappa)$ with $|\tilde{\tilde{\eta}} - \eta_2(\kappa)|$ small, which is shown in Figure 2.5. In this situation we see that the point b is at the right side of the point a.

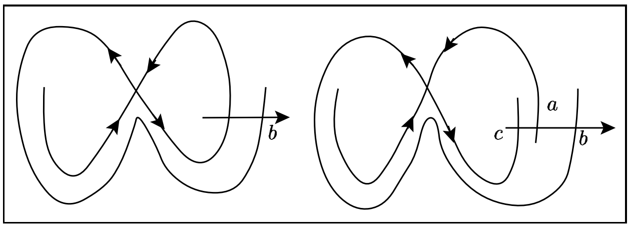

Figure 2.5 *One broken structure of the eight-figure homoclinic orbit.*

Therefore we find that the two branches of stable and unstable manifolds of the eight-figure homoclinic orbit exchange relative position along the crossing section while the parameter η varies from $\tilde{\eta}$ to $\tilde{\tilde{\eta}}$. It follows from the smoothness assumption that there exists a continuous function $\eta = \eta_3(\kappa)$ $(\kappa < \bar{\kappa})$ such that at the parameter value $(\kappa, \eta_3(\kappa))$ equation (2.1) has a big homoclinic orbit.

Similarly we can prove that the other two stable and unstable branches of the eight-figure homoclinic orbit also intersect and perform a big homoclinic at a parameter value $(\kappa, \eta_4(\kappa))$ $(\kappa > \bar{\kappa})$, where $\eta_4(\kappa)$ is a continuous function.

Lemma 2.2 *Assume* **(H1)–(H5)**. *There exist two continuous functions $\eta = \eta_i(\kappa)$ with $\bar{\eta} = \eta_i(\bar{\kappa})$ $(i = 3, 4)$ such that for $\kappa < \bar{\kappa}$ (resp. $\kappa > \bar{\kappa}$) and $|\kappa - \bar{\kappa}|$ small enough, at the parameter value $(\kappa, \eta_3(\kappa))$ (resp. $(\kappa, \eta_4(\kappa))$) equation* (2.1) *has a big homoclinic orbit.*

Remark 2.3 *Just because of the restriction of the method we used here, we can only claim that the curves $\eta_i(\kappa)$ in* Lemma 2.2 *are continuous. We believe that they have the same smoothness as the function f has.*

Summarize Lemma 2.1 and 2.2, we obtain the main results in this paper.

Theorem 2.4 *Assume* (H1)–(H5). *Under small perturbation, from the eight-figure homoclinic orbit there bifurcate two families of small homoclinic orbits and two families of big homoclinic orbits.*

3 Basic numerical methods

In this section we introduce the basic numerical analysis methods for the computation and continuation of homoclinic orbit. Consider the parameterized system

$$\dot{x} = f(x, \kappa, \eta), \quad x \in \mathbb{R}^m, \quad \kappa, \eta \in \mathbb{R}, \tag{3.1}$$

where $m \geq 2$. Assume that at the parameter value $(\bar{\kappa}, \bar{\eta})$ equation (3.1) has a nondegenerate homoclinic orbit $\bar{x}(t)$ with respect to κ.

The fundamental method for computing such orbit pair $(\bar{x}(\cdot), \bar{\kappa})$ was derived by Beyn in his paper [4]. Using projection boundary condition he trancated the homoclinic orbit to a solution of a boundary value problem on a finite time interval, which leads to a well-post problem for fixed $\bar{\eta}$

$$\begin{aligned} &\dot{x} = f(x, \kappa, \bar{\eta}), \quad t \in (-T_-, T_+), \\ &b(x(-T_-), x(T_+)) = (b_-(x(-T_-)), b_+(x(T_+))) = 0, \\ &\Psi(\bar{x}(\cdot)) = 0. \end{aligned} \tag{3.2}$$

Remark 3.1 *1) $T_\pm > 0$ are sufficiently large numbers.*

2) The boundary conditions $b_\pm(x) = 0$ are linear equations such that the zeroes of $b_\pm(x) = 0$ span the stable ($b_+(x) = 0$) and unstable ($b_-(x) = 0$) eigenspaces of $f_x(\xi, \bar{\kappa}, \bar{\eta})$, respectively. This is the so-called projection boundary condition.

3) $\Psi(\bar{x}(\cdot)) = 0$ is a phase condition defined by

$$\Psi(x(\cdot)) = \int_{-T_-}^{T_+} \dot{\bar{x}}^T(t)(x(t) - \bar{x}(t))dt \tag{3.3}$$

Let $x_J(t)$ denote the restriction of the function $x(t)$ ($t \in \mathbb{R}$) on the finite interval $J = [-T_-, T_+]$. Beyn in [4] proved that equations (3.2) have a unique regular solution pair $(\tilde{x}(t), \tilde{\kappa})$ near $(\bar{x}_J(t), \bar{\kappa})$.

We use the arc-length parameter as the continuation parameter and adopt the continuation technique introduced in book [1] to compute the family of regular solutions $(\tilde{x}_\eta(\cdot), \tilde{\kappa}_\eta)$ of equations (3.2) while η varying near $\bar{\eta}$, which approximate the family of nondegenerate homoclinic orbits of equation (3.1). Such method has been successfully used to analyze the global homoclinic bifurcation properties for a valve generator system in [7].

4 Numerical analysis of a chemical system

In this section we will illustrate our main results by a chemical planar system. Consider a parameterized system

$$\begin{aligned} \dot{x} &= -(x^3 - 3x + \eta) - \kappa y, \\ \dot{y} &= x - y, \end{aligned} \tag{4.1}$$

where κ and η are parameters. This system is derived from a chemical reaction model studied in [8]. Guckenheimer studied the global bifurcation properties, including Takens-Bogdanov bifurcation points, saddle-node homoclinic orbits, periodic orbits and other bifurcation phenomena. He proved the existence of an eight-figure homoclinic orbit in this system and provided a local homoclinic bifurcation diagram, see Figure 4.1. In this picture, at the point *dl* equation (4.1) has an eight-figure homoclinic orbit. Along the curves sl_i ($i = 1, 2$) there are small homoclinic orbits bifurcated from the eight-figure homoclinic orbit. And the curve sl_3 represents the parameter values where the big homoclinic orbits occur. He pointed out in the paper [8] that the curve sl_3 transversally passes through the point dl. We will see this is the main difference between his bifurcation diagram and our numerical computation in this paper.

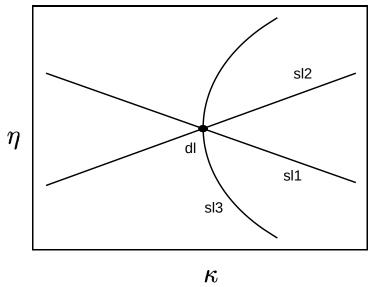

Figure 4.1 *The homoclinic bifurcation diagram derived in* [8].

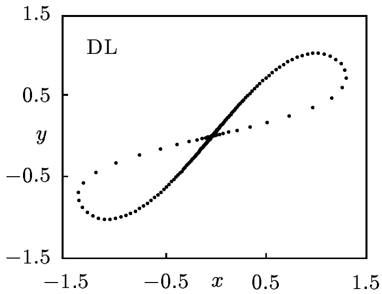

Figure 4.2 *An eight-figure homoclinic orbit detected by numerical method.*

By numerical simulation we find the eight-figure homoclinic orbit (see Figure 4.2) of equation (4.1) at parameter $(\bar{\kappa}, \bar{\eta}) = (2.24106109, 0.00000000)$. Using the numerical method introduced in previous section we find two different shapes of small homoclinic orbits SL_1 and SL_2 (see Figure 4.3) and two different shapes of big homoclinic orbits SL_3 and SL_4 (see Figure 4.4) near this eight-figure homoclinic orbit. The numbers underneath each picture are the (κ, η) value at which we find the corresponding homoclinic orbits.

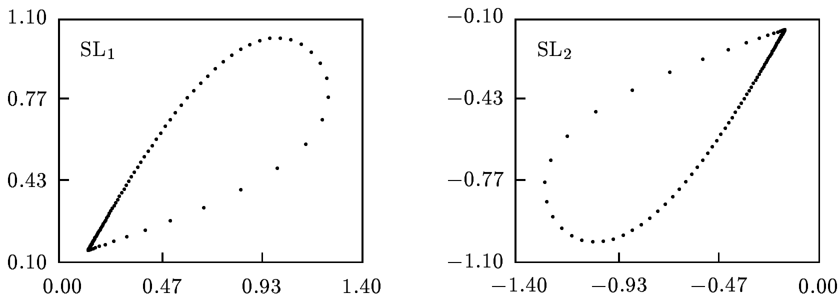

(2.09999981, 0.12627480) (2.09999981, -0.12627480)

Figure 4.3 *The two different shapes of small homoclinic orbits.*

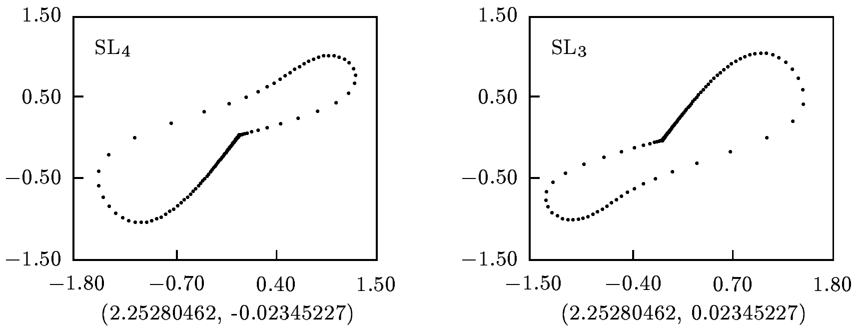

Figure 4.4 *The two different shapes of big homoclinic orbits.*

In next figure we show the computed local homoclinic bifurcation diagram near the eight-figure homoclinic orbit in the parameter (κ, η) plane. Along the curves labeled by sl_i $(i = 1, \cdots, 4)$ there are the corresponding single homoclinic orbits SL_i $(i = 1, \cdots, 4)$ shown in Figure 4.3 and 4.4. In this bifurcation diagram we find two extra bifurcation values tph_i $(i = 3, 4)$, where the big homoclinic orbits undergo turning point bifurcation while doing continuation by parameter κ. Comparing this picture with Figure 4.1 we can easily see the differences: the two curves labeled by sl_3 and sl_4 terminate at the point dl at which they are tangent to the curves labeled by sl_2 and sl_1, respectively.

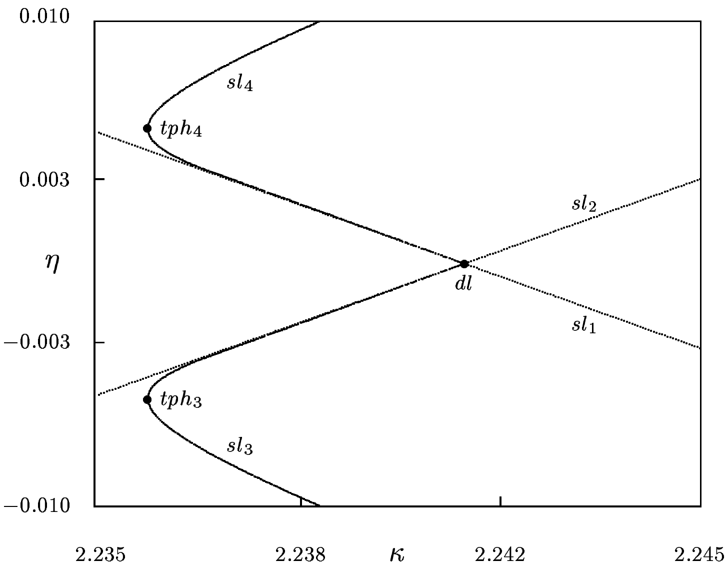

Figure 4.5 *The computed local homoclinic bifurcation diagram near the eight-figure homoclinic orbit.*

References

[1] E. L. Allgower & K. Georg, *Numerical Continuation Methods: An Introduction.* Springer Ser. Comput. Math. **13**, Springer Berlin, 1990.

[2] A. Andronov, E. Leontovich, I. Gordon & A. Maier, *Theory of Bifurcations of Dynamical systems on a Plane.* Israel Program for scientific Translations, Jerusalem, 1973.

[3] D. K. Arrowsmith & C. M. Place, *Bifurcations at a cusp singularity with applications.* Acta Applicandae Mathematicae **2**, 101-138, 1984.

[4] W.-J. Beyn, *The numerical computation of connecting orbits in dynamical systems.* IMA J. Num. Anal. **9**, 379-405, 1990.

[5] F. Dumortier, R. Roussarie & J. Sotomayor, *Generic 3-parameter families of planar fields, unfolding of saddle, focus and elliptic singularities with nilpotent linear parts.* In F. Dumortier, R. Roussarie, J. Sotomayor & H. Zoladek, *Bifurcations of Planar Vector Fields: Nilpotent Singularities and Abelian Integrals.* Lecture Notes in Mathematics **1480**. Springer Verlag, Berlin, 1991.

[6] F. Giannakopoulos & O. Oster, *Bifurcation properties of a planar system modeling neural activity.* Differential Equations and Dynamical Systems, Vol. **5**, No. 3/4, 229-242, 1997.

[7] F. Giannakopoulos, T. Küpper & Y. Zou, *Homoclinic bifurcations in a planar dynamical system.* Accepted by the International Journal of Bifurcation and Chaos.

[8] J. Guckenheimer, *Multiple bifurcation problems for chemical reactors.* Nord-Holland, Amsterdam, Physica **20D**, 1-20, 1986.

[9] J. Guckenheimer & P. Holmes, *Nonlinear Oscillations, Dynamical Systems and Bifurcation of Vector Fields.* Springer Verlag, New York, 1993.

[10] A. I. Khibnik, B. Krauskopf & C. Rousseau, *Global study of a family of cubic Liènard equations.* Nonlinearity, **11**, 1505-1519, 1998.

[11] S. Schecter, *The saddle-node separatrix-loop bifurcation.* SIAM J. Math. Anal. **18**, 1142-1157, 1987.

[12] J. Sotomayor, *Generic bifurcations of dynamical systems.* In M. M. Peixoto (editor), *"Dynamical Systems"*, 549-560, Academic Press, New York, 1973.

[13] S. Wiggins, Global Bifurcation and Chaos (Analytical Methods). Applied Mathematical Sciences, **73**. Springer-Verlag, New York, Berlin, 1988.

[14] S. Wiggins, Introduction to Applied Nonlinear Dynamical Systems and Chaos. Texts in Applied Mathematics, **2**. Springer-Verlag, New York, 1990.

[15] Y.-K. Zou & W.-J. Beyn, *On manifolds of connecting orbits in discretizations of dynamical systems.* In preparation.